EUROPEAN FUSION DEVELOPMENT AGREEMENT

EFDA-JET-CP(05)02-25

D.Testa, T.Bergkvist, D.Borba, C.Boswell, A.Fasoli, T.Hellsten, S.Sharapov
and JET EFDA contributors

Measurement of the Instability Threshold for Toroidal Alfvén Eigenmodes in JET Tokamak Plasmas

Measurement of the Instability Threshold for Toroidal Alfvén Eigenmodes in JET Tokamak Plasmas

D.Testa[1], T.Bergkvist[2], D.Borba[3], C.Boswell[4], A.Fasoli[1], T.Hellsten[2], S.Sharapov[5]
and JET EFDA contributors*

[1]CRPP, Association EURATOM – Confédération Suisse, EPFL, Lausanne, Switzerland
[2]Alfvén Laboratory, KTH, Association EURATOM/VR, Stockholm, Sweden
[3]Associação EURATOM/IST, Av. Rovisco Pais, 1049-001 Lisboa, Portugal
[4]Plasma Science and Fusion Center, Massachusetts Institute of Technology, Boston, USA
[5]EURATOM/UKAEA Fusion Association, Culham Science Centre, Abingdon, OX14 3DB, UK
** See annex of J. Pamela et al, "Overview of JET Results ",*
(Proc.20 [th] IAEA Fusion Energy Conference, Vilamoura, Portugal (2004).

Preprint of Paper to be submitted for publication in Proceedings of the
EPS Conference,
(Tarragona, Spain 27th June - 1st July 2005)

ABSTRACT.
Understanding and controlling the interaction between alpha particles and modes in the Alfvén frequency range is a crucial issue for ITER operation, as these modes can be driven unstable up to amplitudes at which they could cause radial transport of the as themselves. Experimental verifications of the theoretical calculations on the instability threshold of Alfvén Eigenmodes (AEs) driven by MeV-energy ions are therefore needed. In this paper we analyse the dependence of the damping rate and stability threshold of Toroidal Alfvén Eigenmodes (TAEs) on the ion ∇B-drift direction. In addition, the AE decay time at the switch-off of the Ion Cyclotron Resonance Frequency (ICRF) heating power is measured in order to provide for a quantitative comparison with non-linear modelling of the AE interaction with fast ions.

1. TAE STABILITY AS FUNCTION OF THE ION ∇B-DRIFT DIRECTION.

The ion ∇B-drift direction is an important parameter for accessing the high-confinement regime known as H-mode [1,2]. Furthermore, fluid codes analysing the AE damping rate only include equilibrium gradients depending only on the density and temperature, whereas gyro-kinetic codes, such as PENN [3], also make use of ion ∇B-drift terms. As previously reported in Refs.[4,5], the damping rate of n = 1 TAEs is measured to be a factor three larger when the ion ∇B-drift is directed away from the divertor for background plasma parameters (density, temperature and current profile) and eigenfunctions (measured and computed) differing by no more than 30%, which is largely within the uncertainty of the measurements (particularly that for the edge density) and calculations. These differences are not sufficient to explain the variation in the measured γ/ω for n = 1 TAEs, and a convincing theoretical explanation for this data is so far still lacking. Moreover, the limiter discharges used in these studies were largely up-down symmetric, so in principle there should be no net effect from the ion ∇B-drift terms.

A possible explanation for such differences in the measured γ/ω for n = 1 TAEs can however be associated to the observation of different flows at the plasma edge and scrape-off layer for the forward (FBE) and reverse (RBE) ion ∇B-drift directions [6], changing the edge density e-folding length, hence affecting the interaction with the continuum [7]. To provide further insights into this idea, we have considered the experimental measurement of the TAE instability threshold as function of the toroidal mode number. Figure 1 shows the measurement of the AE mode activity for the FBE and RBE case. We note that for the two RBE cases a different spectrum is excited at different levels of P_{ICRF}, due to differences in the background plasma parameters, hence in the damping and drive for the modes. This scatter is then fully reflected in the plot summarising our database, presented in fig.3.

Figure 2 shows the continuum and radial mode structure for the n = 6 TAE calculated with the CSMISH [8] and MISHKA-1 [9] codes, respectively, demonstrating that the continuum and the radial eigenfunction are very similar in the FBE and RBE cases for a representative n = 6 TAE. This also applies for the other modes we have measured, with n in the range n = 1÷10. The continuum

calculations were cut at $\sqrt{\psi_N} = 0.85$ to avoid non-physical results due to the finite number of poloidal harmonics considered.

Figure 3 shows the summary results of our database, which includes 29 RBE and 46 FBE X-point discharges (hence no more up-down symmetric) with a monotonic q-profile, covering a wide range of background plasma parameters (magnetic field, plasma current, density and temperature profiles). The quantity $<\alpha_{FAST}> = -R_0 \int dr[r\kappa(r)\xi_r(r)q^2(r)d\beta_{FAST}(r)/dr] / \int dr[r\kappa(r)\xi_r(r)]$ is a measure of the fast ion drive for the TAE modes. Here $<\alpha_{FAST}>$ is computed at the mode onset and results from an average over the mode displacement $\xi_r(r)$ (as shown in fig.2), to account for the differences in the calculated mode structure. $\beta_{FAST}(r)$ is evaluated using the ICRF power deposition profile calculated from the hot plasma dispersion relation [10]. The value of the calculated $\beta_{FAST}(r=0)$ is also verified against the NPA measurements of the fast ion perpendicular temperature and density, when available. Hence $<\alpha_{FAST}>(n)$ represent the minimum drive from the fast ions that is required to overcome the damping for a TAE with a given n. The scatter in the plot is due to variations in the background plasma parameters (as shown in figs.1B and 1C, for instance), which may also cause differences in the damping rates. The results presented in fig.3 show that the ranges of $<a_{FAST}>$ required to drive TAEs in the FBE and RBE directions overlap significantly as the background plasma parameters are changed throughout this scan. We note however that $<\alpha_{FAST}>(RBE)$ is systematically larger than $<\alpha_{FAST}>(FBE)$. We infer that an $<\alpha_{FAST}>(RBE) \approx (1.3 \div 1.7) \times <\alpha_{FAST}>(FBE)$ is typically required to drive unstable TAEs. Also, this difference in $<\alpha_{FAST}>$ decreases for increasing n's, consistent with the larger γ/ω for n=1 TAEs.

The different flows at the plasma edge and scrape-off layer and the ensuing details of the density and temperature profiles may indeed explain these observations, as inferred from the n = 1 TAE damping rate data. High-n, core localised TAEs will be less affected by edge damping mechanisms than lower n's, which are typically more global modes. Hence the measurement of the difference in the damping rate and the instability threshold for the different ion ∇B-drift directions as function of the toroidal mode number can be used to test the predictions of fluid and gyro-kinetic models of the AE wavefield.

2. TAE DECAY TIME AT THE ICRF SWITCH-OFF

One of the effects determining the AE instability limit in the presence of fast ions is the phase de-correlation between the ICRF and AE wavefield over the ion gyromotion [11]. A piece of information that provides a constraint to the modelling of this effect is provided by the decay of AEs at the ICRF power switch-off, which is observed to occur on time scales much shorter than the fast ion slowing-down time τ_{SD}. Figure 4 shows an example of the measurement of the AE decay time during ICRF modulations and switch-offs: the modes decay over a typical time scale of $\tau_{DECAY} \approx 100 \div 400$ms (depending on the n's), compared to a typical volume-averaged $<\tau_{SD,H}> \approx 600$ms for the ICRF-heated high energy protons driving the modes.

A qualitative theoretical explanation for this phenomenon has been proposed in Ref.[11] (see fig.5B).

Ions interacting with AEs are displaced along characteristics intersecting the resonance surfaces in phase space. In parts of the phase space the distribution function increases with energy along these characteristics and drives the modes, which in turn flattens the distribution function itself. In other parts of the phase space the distribution function decreases with energy along the characteristics, which leads to a damping of the mode by the fast ions themselves. ICRF heating can partially restore the inverted distribution function on a longer time scale, leading to a non-linear oscillation of the mode energy, which appears as a splitting of the Fourier-decomposed signal, as previously observed for the *pitchfork splitting* [12].

As the ICRF heating is turned off, the restoration of the inverted distribution function ceases and the AE is damped out by wave-particle interactions from the stable part of the distribution function. To provide for a quantitative validation of this theoretical model, 43 JET discharges with a monotonic q-profile have been analysed to compute the AE decay time from the measured time evolution of the mode amplitude A(t). In Eqs.(1A, 1B) below the ICRF heating is switched-off at $t = t_0 = 0$, with $P_{ICRF} = 0$ at $t = t_1$ using a linear ramp-down, H(x) is the Heaviside function, Q(t) is the time-integrated fast ion drive. Equation (1A) was solved iteratively: a first guess for t_{DECAY} is obtained from $A(t) \propto \exp(-t/\tau_{DECAY})$, which is then used to evaluate the left-hand side of Eq.(1A) using Q(t), hence A(t). We then iterate until convergence at the 95% confidence level is reached, usually within 2-4 iterations.

$$A(t) = A(t=t_0)e^{\frac{t}{\tau_{DECAY}}} + Q(t)\tau_{DECAY}\left[\left(1+\frac{\tau - t}{t_1}\right)e^{\frac{t}{\tau_{DECAY}}}\, H\left(1-\frac{t}{t_1}\right)\right], \qquad (1A)$$

$$Q(t) = \int_0^1 dx\xi_r(x,t)\,xk(x,t)\int_{t_0}^{t} dt'\alpha_{FAST}(t',x) \Big/ \int_0^1 dx\xi_r(x,t)\,xk(x,t). \qquad (1B)$$

Figure 5A shows the summary result of our database: the scatter indicates the measured range of $\tau_{DECAY}/\langle\tau_{SD,H}\rangle$ (here the average is over the mode radial structure) for the different plasma conditions (shape, current, density and temperature profiles) analysed in this work. We notice that $\tau_{DECAY} \approx \langle\tau_{SD,H}\rangle/3$, and it is larger for $n = 5 \div 7$ modes. The relative roles of MHD modes in flattening the fast ion distribution function on time scales shorter than t_{SD} compared to the ICRF-induced diffusion can be analysed based on these observations. Reproducing this measured n-dependence becomes in particular the crucial point for validating quantitatively the theoretical model of Ref.[11]. Such detailed quantitative comparison with numerical modelling is now in progress and will be reported in future work.

ACKNOWLEDGEMENTS

This work has been conducted under the European Fusion Development Agreement. D.Testa and A.Fasoli were partly supported by the Fond National Suisse pour la Recherche Scientifique, Grant 620-062924. C.Boswell was partly supported by the DoE contract No. DE-FG02-99ER54563.

REFERENCES

[1]. W.Suttrop et al., PPCF **39** (1997), 2051.

[2]. Y.Andrew et al., PPCF 46 (2004), 337.

[3]. A.Jaun et al., PPCF **43** (2001), A207.

[4]. D.Testa et al., PPCF **46** (2004), 1.

[5]. D.Testa et al., Paper EX/P4-45, 20th IAEA, 2004.

[6]. R.Pitts et al., JNM337 (2005), 146; S.Erents et al., PPCF **46** (2004), 1757.

[7]. G.Fu and H.Berk, private communication, 2005.

[8]. G.Huysmans et al., PoP8 (2001), 4292.

[9]. A.Mikhailovksi et al., PPR **23** (1997), 844.

[10]. D.Testa et al., PoP6 (1999), 3489 and PoP6 (1999), 3498.

[11]. T.Bergkvist et al., NF **45** (2005), 485.

[12]. A.Fasoli et al., PRL **81** (1998), 5564.

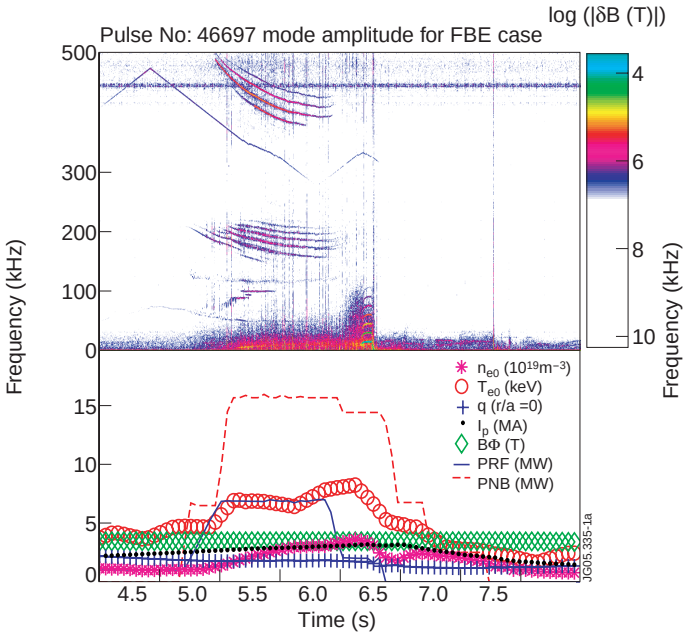

Figure 1(a): Measurement of the AE activity for the FBE case Pulse No: 46697: even with $P_{NBI} \approx 6.5$MW, the n = 4 TAE is unstable at $P_{ICRF} \approx 3.5$MW.

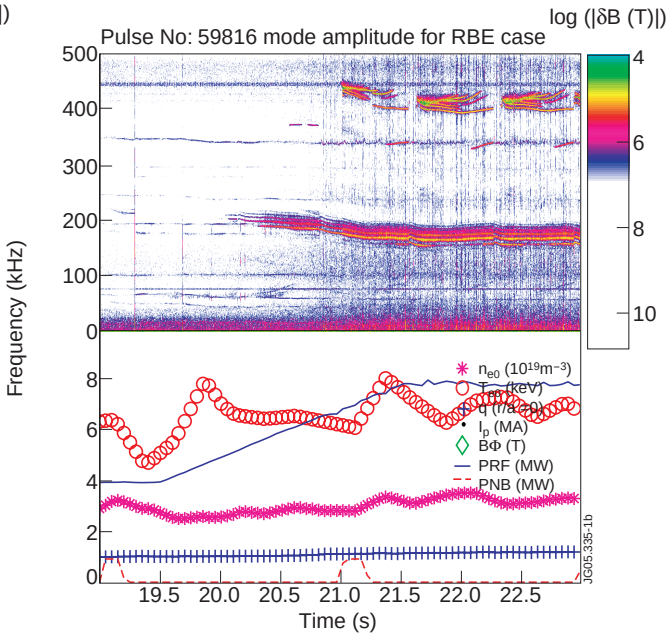

Figure 1(b): Measurement of the AE activity for the RBE case Pulse No: 59816: here the n = 5 TAE becomes first unstable at $P_{ICRF} \approx 5$MW.

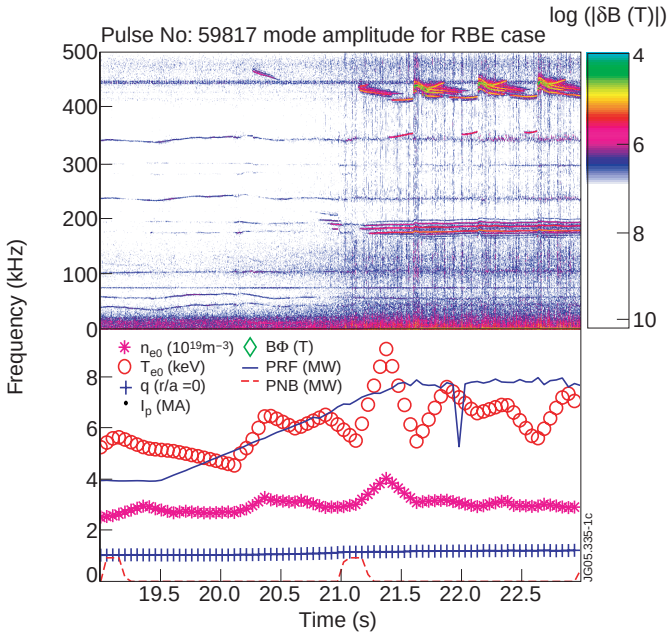

Figure 1(c)Measurement of the AE activity for the RBE case Pulse No: 59817: here the n = 8 TAE becomes first unstable at $P_{ICRF} \approx 6.5$MW.

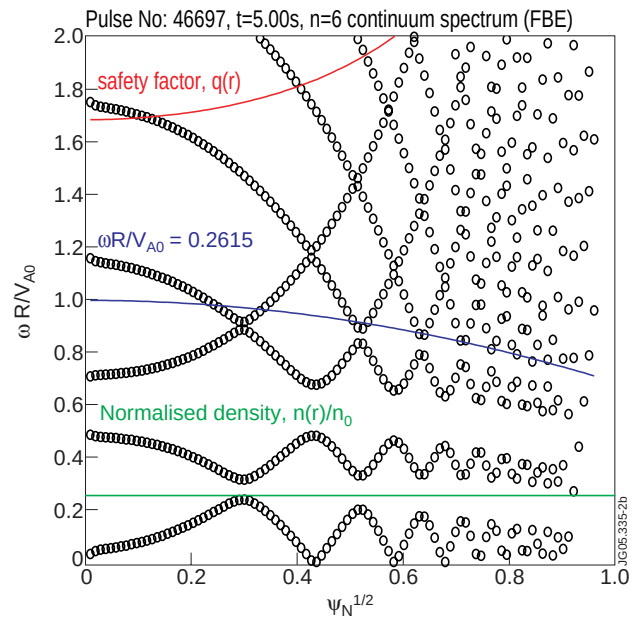

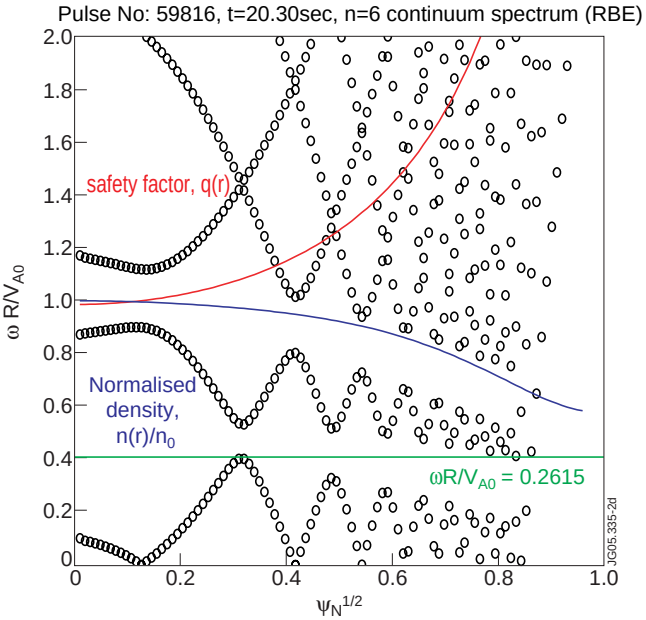

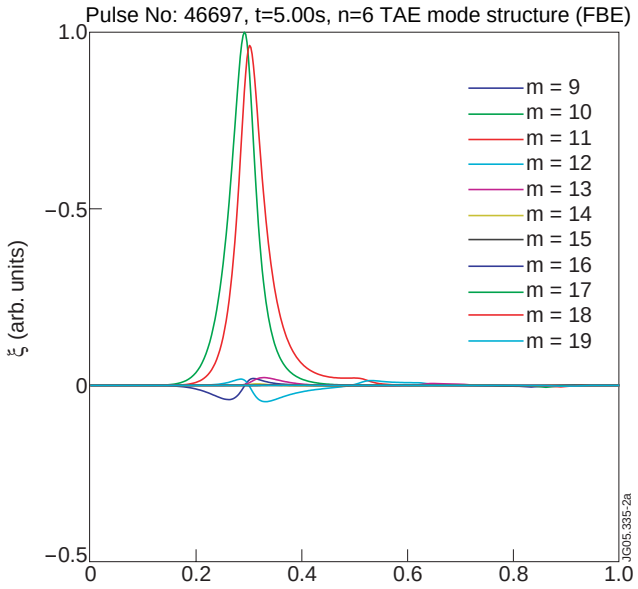

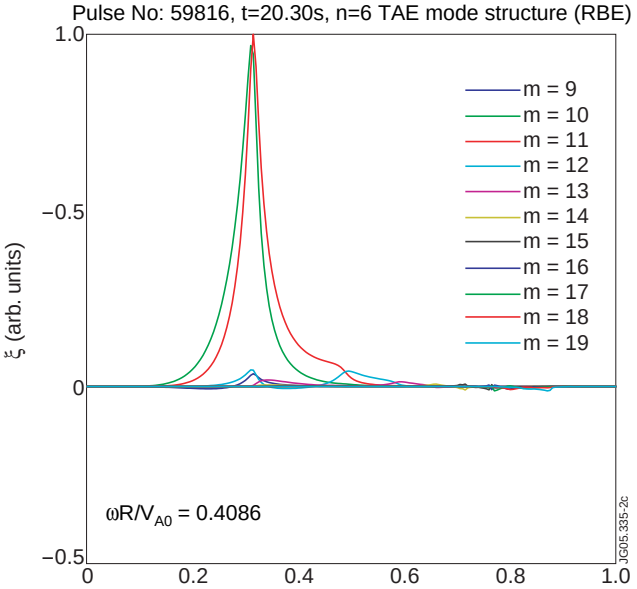

Figure 2: (a) Continuum and radial mode structure calculated for the n = 6 TAE for Pulse No: 46697 at t = 5.00sec.

Figure 2: (b) Continuum and radial mode structure calculated for the n = 6 TAE for Pulse No: 9816 at t = 20.30sec.

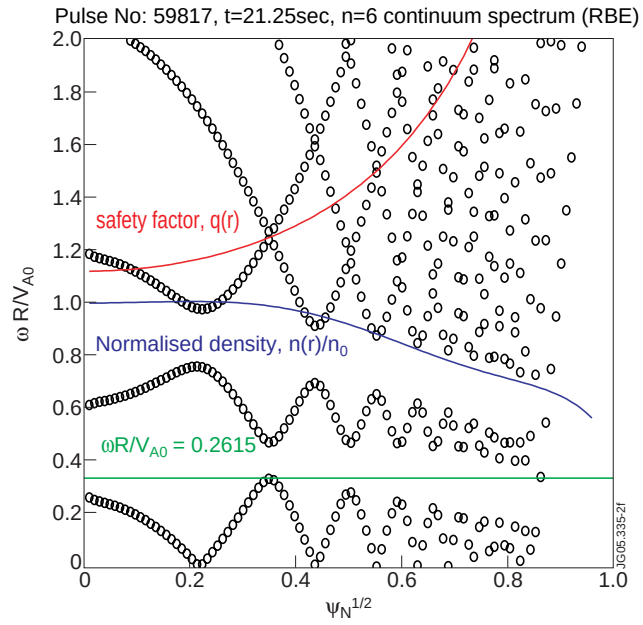

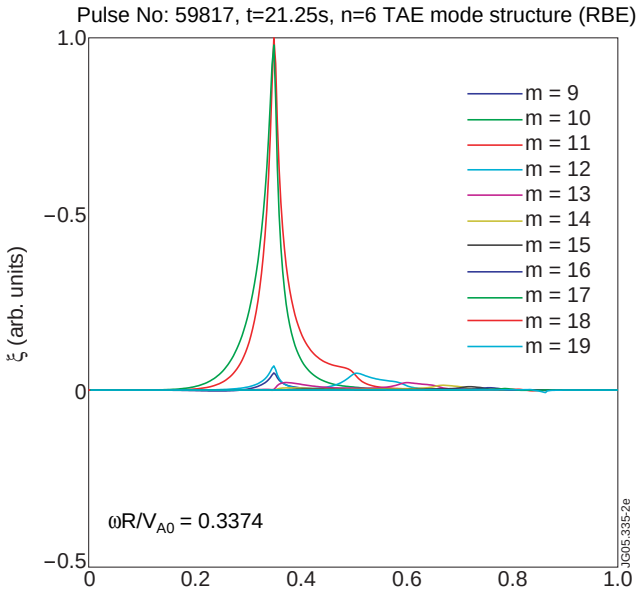

Figure 2: (c) Continuum and radial mode structure calculated for the n = 6 TAE for Pulse No: 59817 at t = 21.25sec.

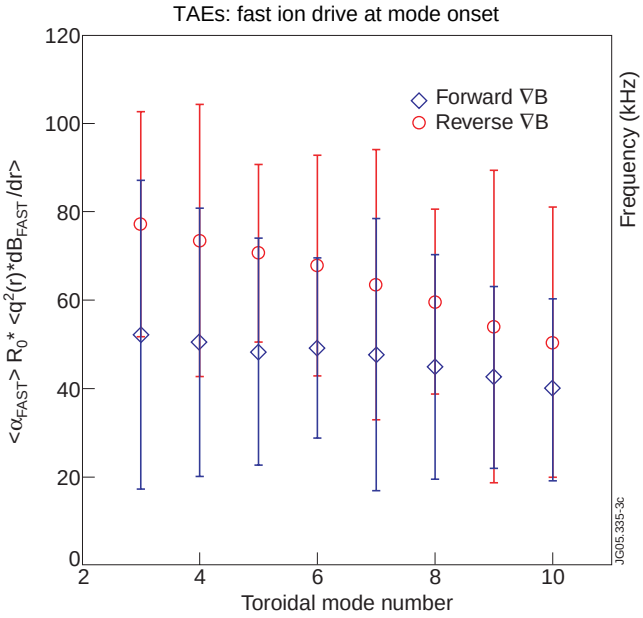

Figure 3: TAE instability threshold as function of the ion ∇B-drift direction for different n's.

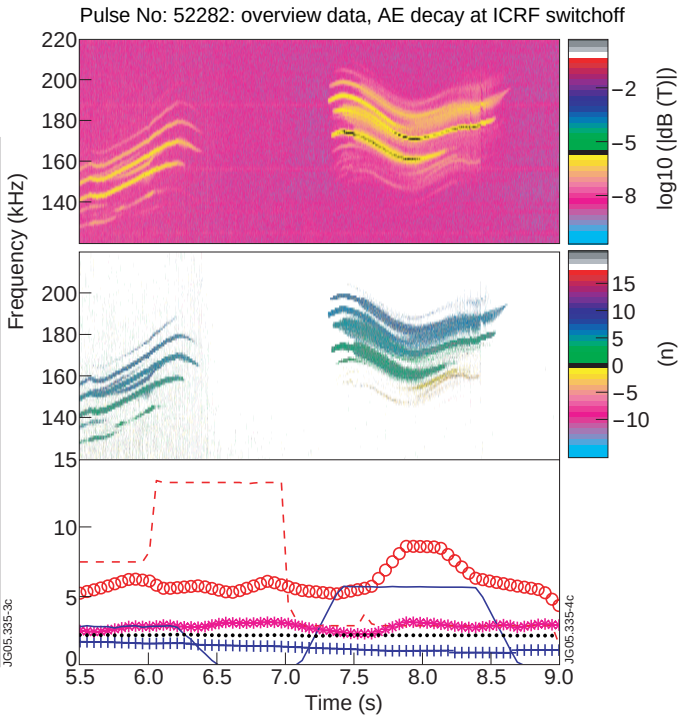

Figure 4: Decay of TAEs and EAEs at constant P_{NBI} during a modulation of the ICRF power for Pulse No: 52282.

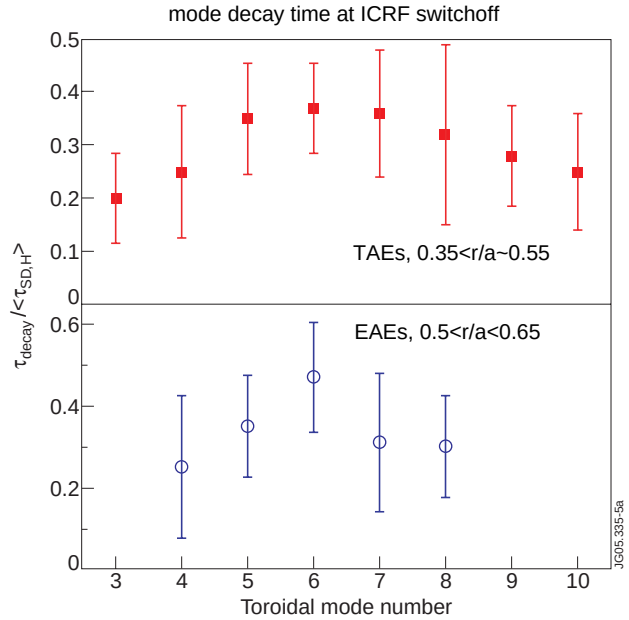

Figure 5: (a) Decay time for TAEs and EAEs at the ICRF power switch-off (or ramp-down) as function of n's (<$\tau_{SD,H}$> is averaged over ξ_r). Note the dependence over the n's, with τ_{DECAY} longer for n = 5÷7 AEs.

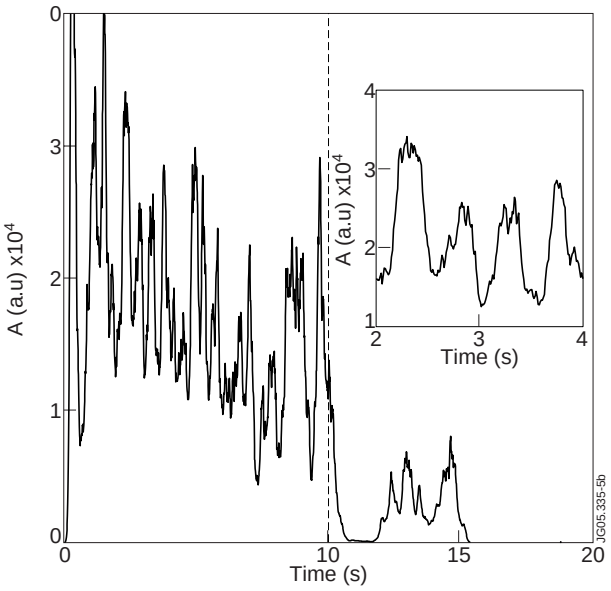

Figure 5: (b)Simulation of the mode amplitude during ICRF with the SELFO code [11]. As the ICRF is turned off at t=10ms, the mode decays over 0.3ms, much faster than t_{SD}. Later bursts occur due to partial restoration of the distribution function by collisions. A zoom of the mode oscillations is shown for 2<t(ms)<4.